

Dynamic Modelling of Commercial Aircraft Secondary Flight Control Systems

Graham Hardwick and Isabella Panella

Systems Engineering, UTC Aerospace Systems, Stafford Road, Wolverhampton, U.K.

Keywords: Commercial, Aircraft, High-lift, Secondary, Flight, Controls, Systems, Mathematical Modelling, Design.

Abstract: This paper describes the use of mathematical modelling within secondary flight control systems for commercial aircraft. The modelling process is described from generation of model requirements, model management through to model validation. The paper describes an example of a parametrised high-lift system model developed in Simulink. Analyses of the model outputs are provided and a sensitivity analysis is performed on a selected design parameter. This work highlights the advantages of integrated modelling to support the conceptual design phase within the lifecycle system design process.

1 INTRODUCTION

Commercial aircraft utilise secondary flight control surfaces, such as flaps and slats to modify the wing profile in order to increase aerodynamic lift for a given air speed. This allows aircraft landing speeds/distances to be reduced. The “high-lift” system is often an alternative definition used in the aerospace industry to refer to secondary flight control system actuation.

UTC Aerospace Systems design, manufacture, and integrate secondary flight control systems for a variety of commercial aircraft, from wide body to single aisle configuration, from business jets to the A380.

This paper describes the use of mathematical modelling of the secondary flight control system at UTC Aerospace. System modelling tools are utilised from the proposal/concept stage all the way through system design, development, manufacturing, system integration, and in service-conditions.

Due to the long timescales of commercial aircraft project lifecycles the models need to be:

- Appropriate to application. For example pseudo dynamic modelling is used for static size case development or fully dynamic so that transient dynamics can be interrogated.
- Modular and documented. Due to programs spanning over decades, technologies and modelling capability will evolve and the model

will need to be modular and well documented in order to support future updates.

- Refer to requirements. Model requires appropriate referencing to requirements where appropriate.
- Version controlled so that configuration of the model can be accessed and co-ordinated with the correct design build standard of the hardware.
- Verified using unit, subsystem and system physical tests.

The validation and verification system design process is a legacy approach in system design and within the aerospace industry has been endorsed within the standards defined in ARP4754A, 2010, SAE International. Systems engineering utilises Model Based Design within the systems Validation and Verification cycle as a core instrument to guarantee robustness and integrity within the systems, as reported in INCOSE.

The validation and verification processes based on modelling and simulation have been further detailed in Figure 1, whereby iterative cycles of validation and verification for each stage are highlighted. This process is followed for the implementation of the functional high lift system. The work herein presented details the iterative nature of the preliminary design stage of a product life cycle. Referring to figure 1, this paper explores the first level of iteration which enables to derive a functional framework from customers’ requirements

through a process of requirements allocation and elicitation implemented through modelling and simulation, specifically through:

- Sensitivity studies
- Trade off analysis
- Test case development
- Decomposition of requirements

The engineering product development schedule is superimposed with the validation and verification

process to highlight the stages where MBSE can add value.

In general, model based design emphasises the use of models through the entire life cycle such as developing test cases and aiding verification activities, generating prototype control code, supporting solving problems, as well as for hardware in the loop activities and also supporting certification activities.

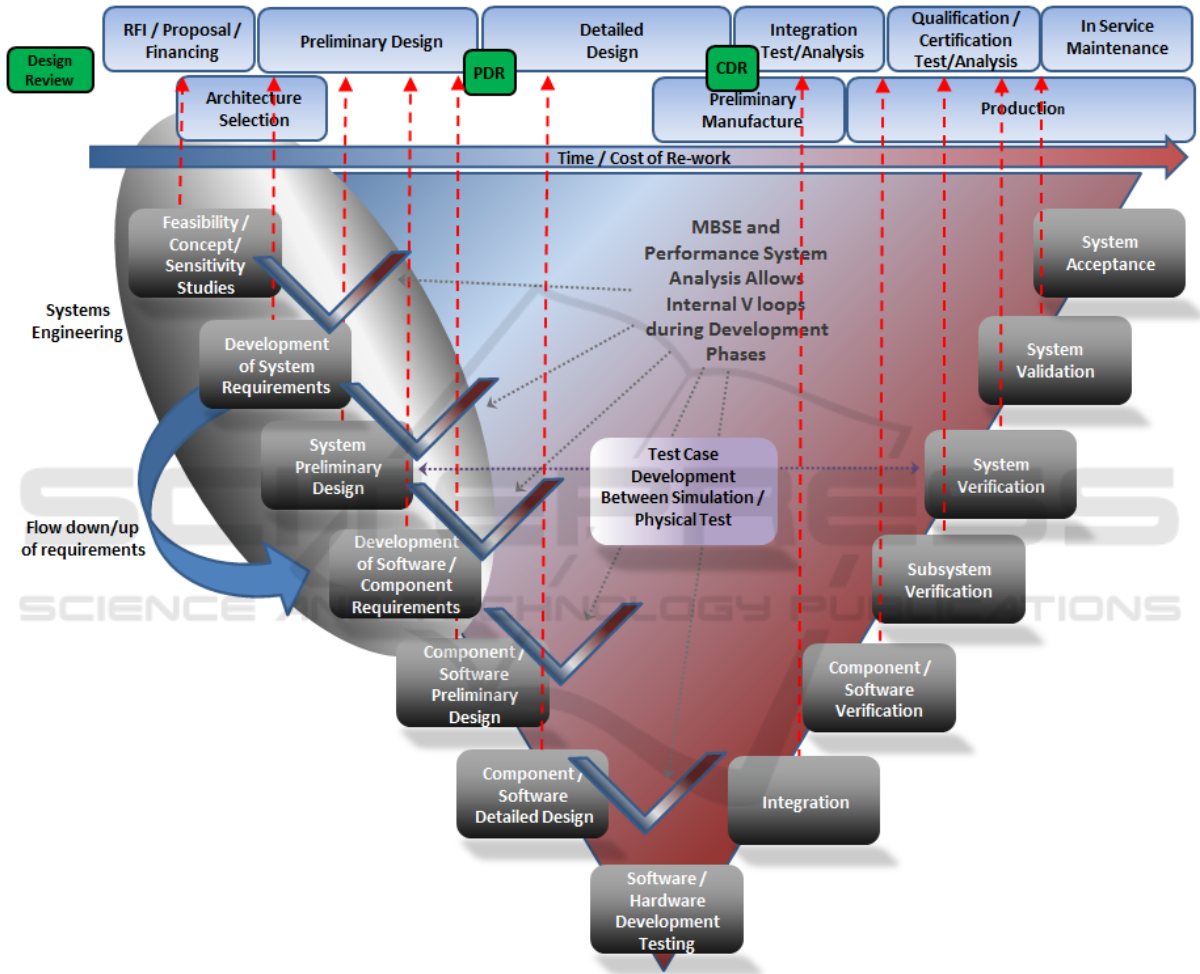


Figure 1: Validation and Verification System Design Process.

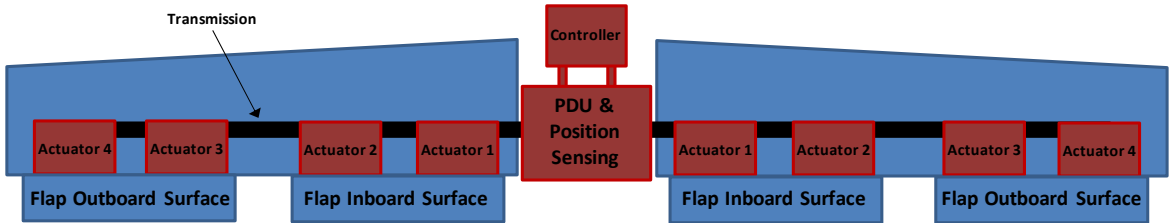


Figure 2: High Lift architecture.

2 HIGH LIFT FUNCTIONAL ARCHITECTURE

The following describes the High Lift Functional architecture. The architecture shown in Figure 2 is the result of a previous study presented in Hardwick, Hanna, and Panella, 2017. It describes a generic medium sized commercial aircraft flap system, characterised by a single transmission line and distributed actuators spaced symmetrically with respect to the aircraft centreline. This architecture presents only a flap system and does not include the slat actuators.

The physical layout includes elements of the functionalities that a high lift system needs to present which are:

- Central source Power Drive Unit (PDU) which provides the power drive actuation to the system and has position sensing capability; This interfaces with the secondary flight controller for control and monitoring functions. The PDU is dual channel for redundancy. Hydraulic valves are controlled by the flight controller and regulate the flow to the hydraulic motors. The motors drive a mechanical gearbox that drives the transmission.
- Transmission shafts connect the PDU to the actuators on the wing and hence enabling synchronous movement of both wings.
- Mechanical wing actuation with four rotary geared actuators (RGA) per wing; These contain gearboxes which provide mechanical advantage to the transmission drive torques. This enables the transmission to drive aerodynamic loads with large torques.
- The secondary flight control system interfaces with the PDU, sensors and safety devices which arrest the system during failure case scenarios. It also interfaces with the main aircraft flight controller.

3 MATHEMATICAL MODEL

Herein, the mathematical model of a High Lift System is described and mapped into a Simulink model, which is then described.

The model is used to perform a sensitivity study to support optimal design point for the selection of the PDU, considering as the key parameter its gear ratio. A discussion of the model verification is also presented.

The first step is to define the model requirements. Requirements enable the definition of the overall performance requirement for the system, operational and environmental conditions, as well as regulatory considerations are needed to ensure safety. They set the “boundary conditions” for the systems, which will need to be validated and verified.

It is important to consider another constraint when implementing a simulation model. The model complexity is proportional to run time. Therefore, the model fidelity needs to be traded with the speed of simulation that we want to achieve.

Once the requirements are defined, specific performance descriptions need to be allocated to the functional blocks, and model outputs are linked to the systems requirements, such as:

- Flap system deployment times;
- Flap system hydraulic flow rate;
- Dynamic and steady state transmission loads;
- PDU normal operating velocity.

Dynamic modelling has been achieved through the application of first order differential equations.

These equations are represented in the form of a state-space model within the Simulink modelling environment, which utilises a non-stiff variable step ordinary differential solver (ODE). The model contains continuous states but the governing equations are non-linear and hence the system is a non-linear time invariant system. State space modelling is a control systems technique to represent the dynamic behaviour of a system as reported in ZadehandDesoer, 1963.

3.1 Model Architecture

The functional architecture is now mapped into the simulation environment through the application of mathematical equations capturing the individual functions’ behaviour, according to mechanical, hydraulic and electrical physics laws.

Examples of the equations used to create the blocks are provided in the following sections.

The principle of operation is the following. Mechanical transmission blocks connect the PDU to the actuators. The drive to the PDU is generated by transferring hydraulic power into mechanical using hydraulic motors.

Figure 3 highlights the system architecture mapped into a Simulink model. This contains the following subsystems:

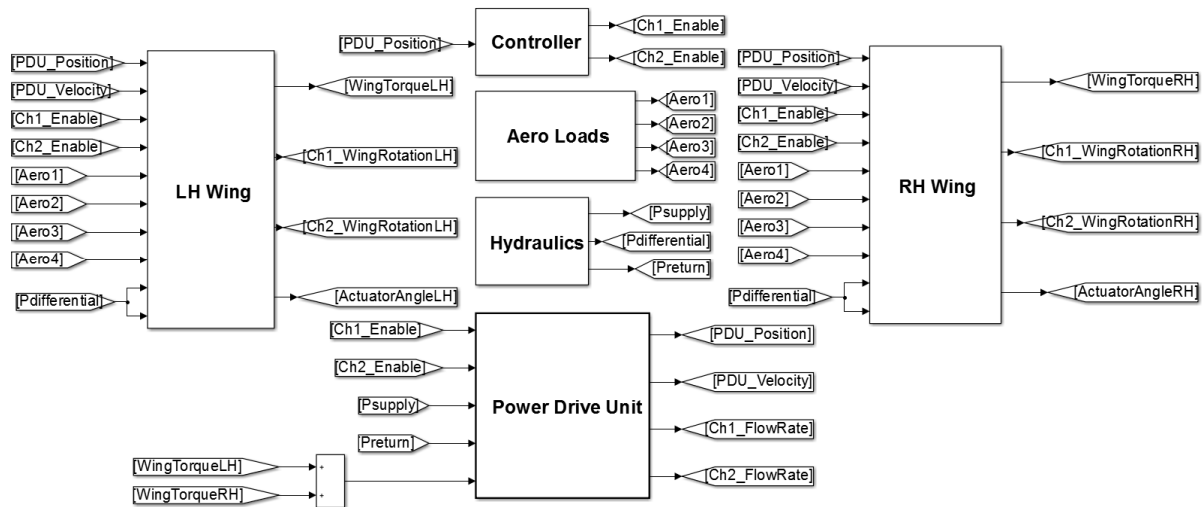


Figure 3: Model architecture of a generic secondary flight control system in Simulink.

- “Controller” is the Secondary flight controller (which contains I/O to the aircraft controller);
- “Power Drive Unit” is the Dual channel power drive unit;
- “LH and RH Wing” are the two mechanical wings containing the high lift system;
- “Aero Loads and Hydraulics” are the interface definition of the aerodynamic loads and hydraulic system.

The PDU and the controller (figure 2) are translated into the Simulink diagram (figure 3) and are connected using “GoTo” blocks for example:

- Ch1(2)_Enable – controller to PDU enable electrical signal.
- PDU_Position – PDU to controller position
- Aero1(n) – Aerodynamic loads between the interface and wings
- Psupply – Hydraulic supply pressure between interface and PDU

3.2 High Lift Transmission

The high lift transmission wing subsystems are modelled as mechanical blocks that include component stiffness, inertia, damping, transmission efficiency and drag. These blocks are defined as “LH Wing” and RH Wing” in figure 3. A portion of these blocks have been expanded in figure 4.

Each inertia element contains one dimensional rotational states (accelerations / velocities). For example the equation to convert relative transmission shaft deflection (dx) and velocity (dv)

into a transmission torques is modelled as follows (where k_{trans} and c_{trans} are the respective torsional stiffness and damping of the transmission):

$$\text{Shaft Torque} = k_{trans} * dx + c_{trans} * dv \quad (1)$$

Figure 4 provides the Simulink model of the transmission system including shafts and flap panels showing the connections between the Simulink blocks. The shaft torque is multiplied by a transmission efficiency η_{trans} that calculates the downstream torque for example:

$$\text{Output Torque} = \text{Input Torque} * \eta_{trans} \quad (2)$$

All shaft torques attached to the panel are summated and then integrated with the aerodynamic loads into the flap panel dynamic model. This process is repeated down the transmission line. The transmission torque and aerodynamic loads are inputs to the flap panel block.

The net torque acting on the flap panel (T_{flap}) is calculated as follows. The aerodynamic loads (T_{aero}) are converted into the transmission torque reference frame using the actuator gear ratio (G_{act}) and mechanical efficiency (η_{act}). This is summed with the torque from the transmission shafts (T_{trans}) and drag (T_{drag}) is deducted which is described in equation 3:

$$T_{flap} = (\eta_{act} * T_{aero} / G_{act}) + T_{trans} - T_{drag} \quad (3)$$

The model contains additional complexities for example determining the direction of the drag torque dependant on the direction of rotation.

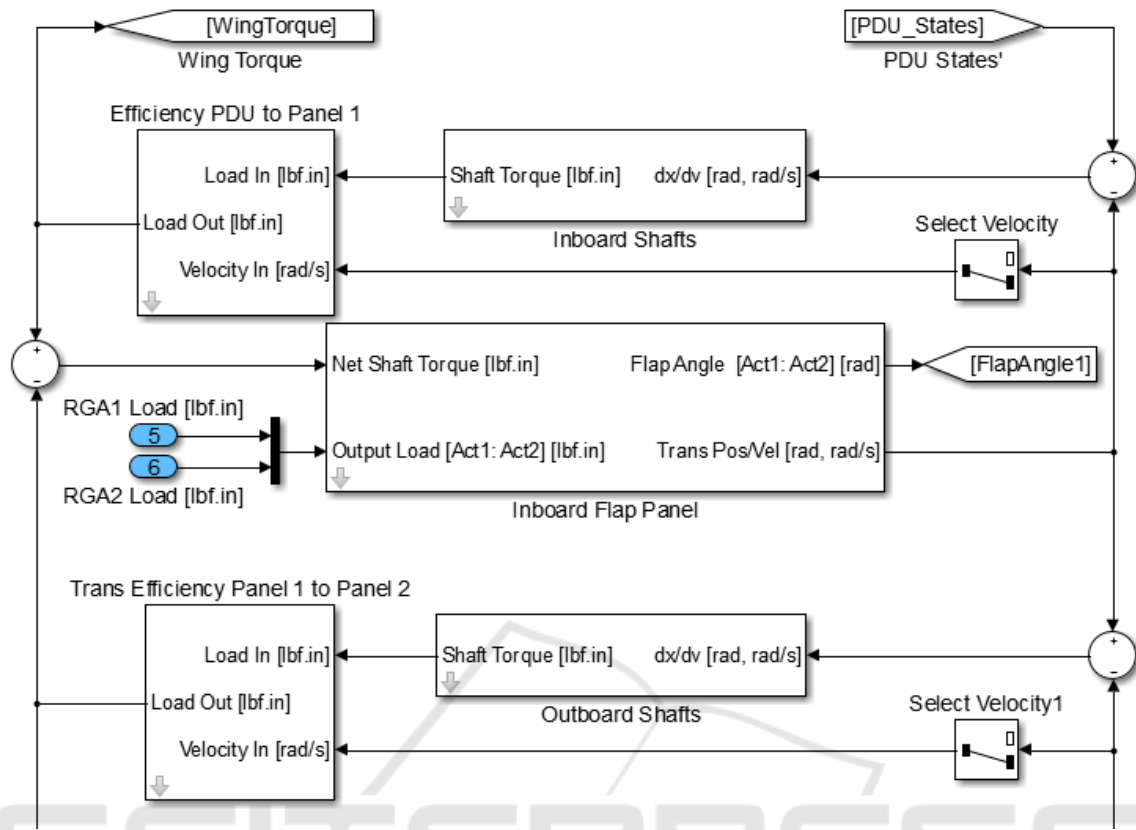


Figure 4: Model of High Lift system in the wing.

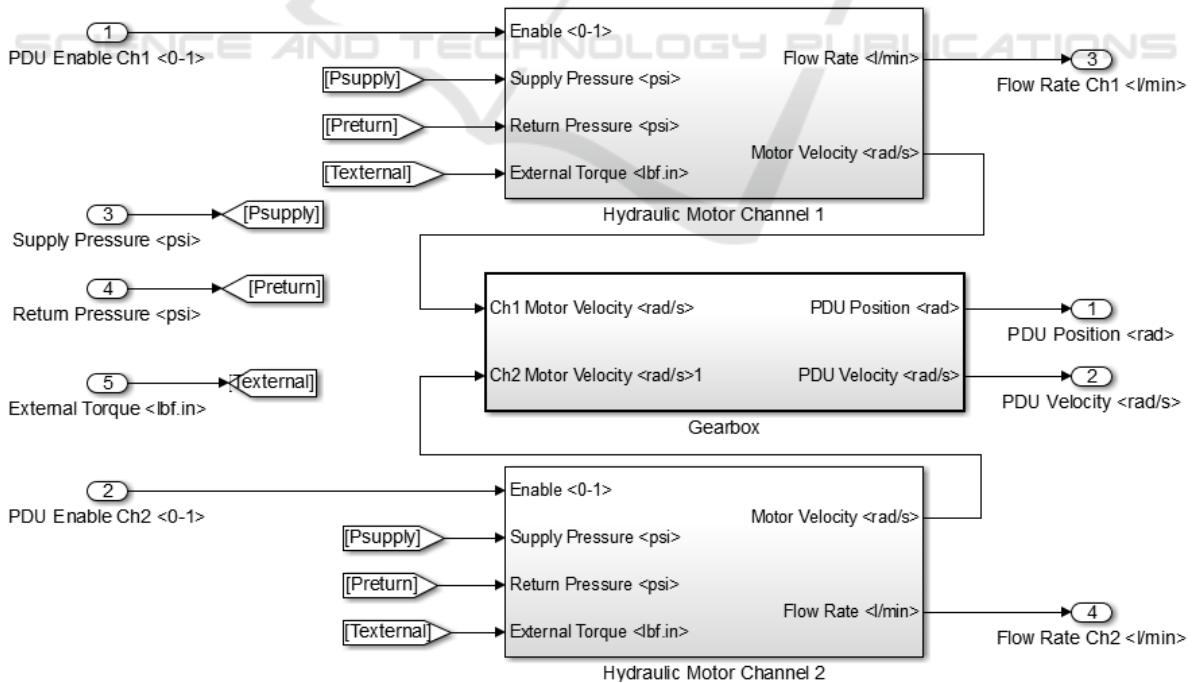


Figure 5: Power Drive Unit Model.

The net torque on the flap panel (T_{flap}) is converted into panel acceleration (A_{flap}) by dividing by the inertia of the panel and transmission components (I_{act}).

$$A_{flap} = (\eta_{act} * T_{flap} / I) \quad (4)$$

The velocities and displacements are then determined by integrator blocks.

3.3 Power Drive Unit

The power drive unit model incorporates two hydraulic channels that contain a constant displacement motor and control valve to activate the motor. More complex hydraulic control arrangements can be used to control the power drive unit more precisely such as electro hydraulic servo valves.

This block is defined as “Power Drive Unit” in figure 3 and has been expanded in figure 5.

The PDU enable signal controls both the brake in the PDU and the control valve. The control valve dynamics are represented by a first order transfer function using the time constant T_c :

$$\text{Valve Transfer Function} = 1/(1 + T_c(s)) \quad (5)$$

Movement of the control valve determines the pressure drop across (ΔP) the motor. The pressure drop is converted to a motor torque (T_m) by multiplying by the motor displacement (K_{mot}) and incorporating drag (T_{drag_m}) and motor efficiency (η_{mot}) as shown by equation 6:

$$T_m = \Delta P * K_{mot} * \eta_{mot} - T_{drag_m} \quad (6)$$

Hydraulic motor acceleration is calculated by dividing the motor torque by the motor inertia. Integrating the acceleration provides the angular velocity of the motor. Both motor speeds are transferred through a gearbox where the PDU output shaft position and velocity states are passed to the wing.

3.4 Secondary Flight System Controller

The secondary flight control opens the control valve and releases the system brakes when the position demand is not equal to the present PDU position. When the system reaches target position the control valve is closed and all brakes are engaged.

Multiple brakes are often used in high-lift systems due to the transmission disconnect failure

scenarios. When activated the brakes prevent excessive asymmetry between the left and right hand wing. An actual high-lift controller will typically have a number of sensors to monitor certain failure conditions and arrest the system before they become catastrophic. However, for the purposes of this paper these are omitted.

3.5 Model Parameters

A list of the model parameters is provided in the appendix and these are set via the use of Matlab functions. This allows multiple model parameters to be run through batches. All parameters used in the model are arbitrary and do not relate to a particular aircraft. The model outputs are used to assess the operating speed of the system and resulting deployment times. The transmission loads generated is also analysed.

4 RESULTS

4.1 Time Histories

The basic output from the model is logged in time histories. Figure 6 highlights the PDU output shaft velocity during deployment.

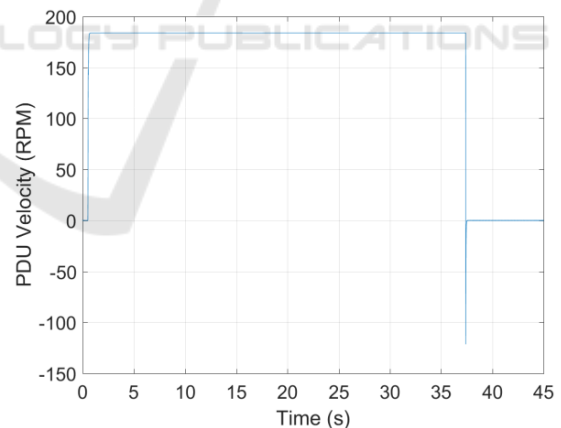


Figure 6: Time history of PDU output shaft velocity.

This shows that when the system proceeds at a normal operating speed of 184 rpm. It takes approximately 36.9s to fully deploy the system from the stowed condition.

Both hydraulic motors consume approximately 12.6 l/min flow rate during operation as provided by figure 7:

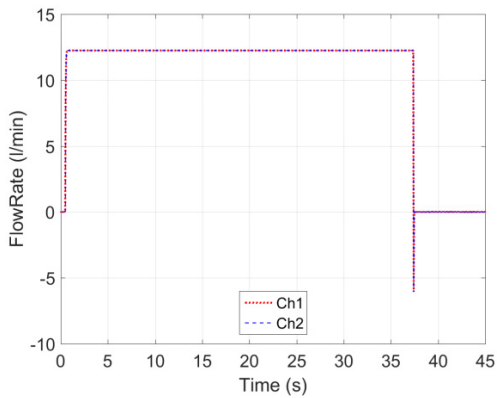


Figure 7: Hydraulic motor flow rate consumption.

The following time history shows the system position at both the PDU and the wing tips. It can be seen that the wing tips marginally lag the PDU. The lag is due to stiffness of the transmission system and it is the expected systems behaviour.

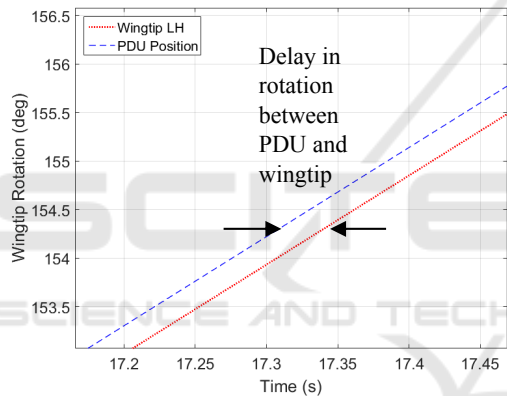


Figure 8: System Position at the PDU and wing tip sensors.

Finally the transmission torque from each wing can be plotted. This shows an initial transient peak torque at 97Nm reducing to a steady state torque of 93Nm per wing.

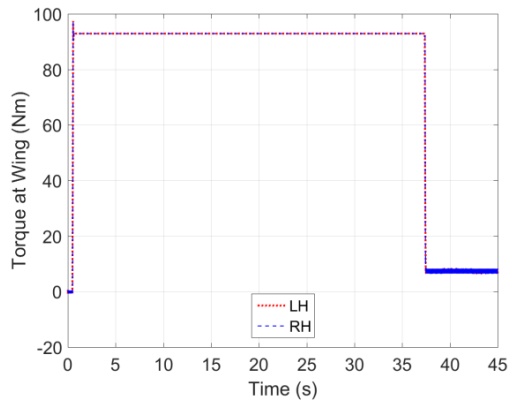


Figure 9: Wing torques during deployment.

4.2 Sensitivity Study

The model parameters have been fed into the model as ranges in order to assess the systems sensitivity. The example provided shows how the gear ratios of the PDU gearbox can be modified to achieve various system requirements such as:

- Minimise running and peak transmission torques;
- Minimising the hydraulic flow rate consumption;
- Reducing deployment time.

Figure 10 provides the results from a batch of simulations where the PDU gear ratio was varied between 20:1 to 30:1.

The results from the simulations indicate the optimal gear ratio to be 26:1 which maximises operating speeds and hence reducing deployment times. An optimum occurs because of the trade-off between the mechanical advantage of the PDU and the drag which increases as function of speed.

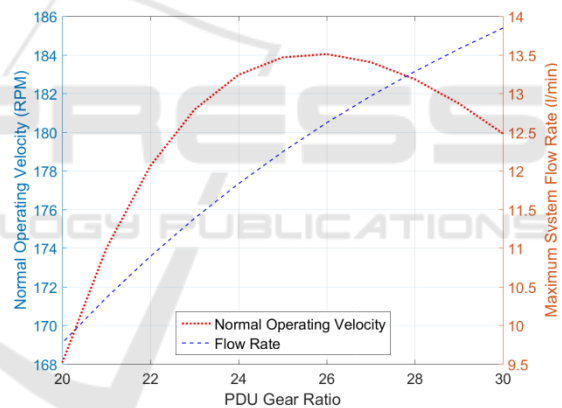


Figure 10: Operating velocity and flow rate vs gear ratio.

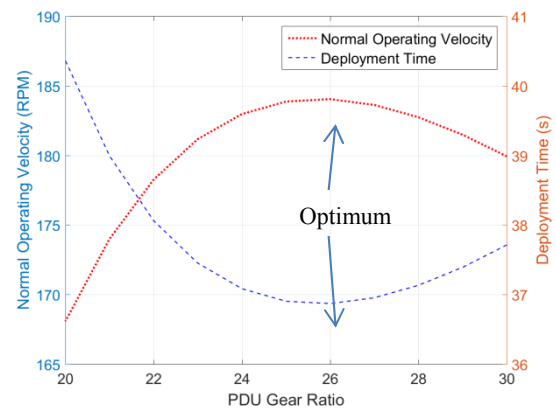


Figure 11: Normal operating velocity and deployment time vs gear ratio.

At low gear ratios the PDU has a lower mechanical advantage and hence the PDU's torque capability is lower, which implies lower operating speeds. At high gear ratios the motor speed is higher for a given PDU output speed and the speed induced drag in the motor increases and limits the PDU speed.

Figure 11 presents the sensitivity analysis of the variation of the PDU ratio vs. the normal operating velocity (blue line) and the PDU gear ratio vs. the deployment time. The optimal gear ratio is the one defined by the value for which we have operating velocity and minimum deployment time. In this example, the optimum PDU gear ratio for this system is 26:1. The transmission torques generated by the model can be used to as an input into stress sizing simulations. Figure 12 shows that the running torques in the transmission are highest at 26:1 due to the highest operating speeds. The peak transmission torque has a marginally different trend due to the dynamic transmission characteristics.

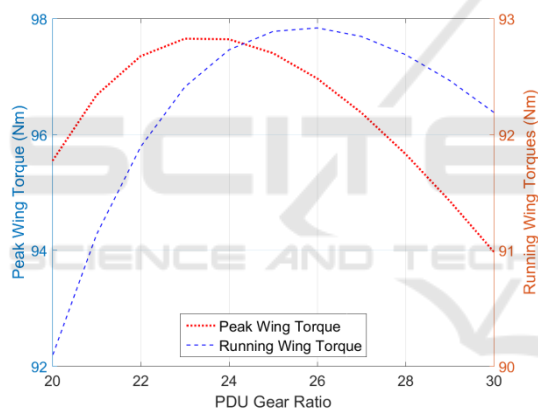


Figure 12: Peak and running torque in the wing transmission vs gear ratio.

A hydraulic high lift system is typically sized based upon cold temperature operating and breakout performance. The reason behind it is that the drag in the transmission is at the highest while the PDU capability is the lowest.

5 MODEL VERIFICATION

The mathematical models provided herein have been verified against physical test data. This has provided the confidence to use the model outputs to support the design and development of numerous high lift aircraft systems.

Model verification has been performed at numerous stages of the system engineering process for example at component level (actuator, PDU etc.) and against full system rig and simulated results.

Excellent model correlation has been achieved at both individual component and full system level over a range of environmental temperatures, aerodynamic loads across multiple programs.

Models have been further utilised in software and hardware in the loop environments with suppliers and customers.

Models of secondary flight control systems developed in the Simulink environment have been rapid prototyped to support hardware in the loop simulation.

This has provided the following benefits:

- Development time of software algorithms significantly improved;
- Control models tested in simulation prior to integration on the test rigs improve systems' robustness and easiness of integration.
- Use of the mathematical model as a precise implementation of the controller and thereby reducing misinterpretation of formal requirements.

In recent years there has been a significant shift in the aerospace industry to move from rig tests to modelling and simulation environments. Simulations allow testing of the system in extreme cases that test rigs may not be able to perform due to:

- Too dangerous/expensive to perform;
- Not possible to perform such as all system tolerances being maximised/minimised;
- Limitations of the test rigs.

6 CONCLUSIONS

This work has described the modelling process of a commercial aircraft high-lift transmission and power drive system. An example model was provided that was developed in the Simulink modelling environment and results of a sensitivity analysis have been provided. Model validation has been discussed together with the integration of models into other engineering environments.

This paper provides a generic functional model and demonstrates the analysis techniques used within the design and development of high lift systems that are in-service.

REFERENCES

- Hardwick, G., Hanna, S., Panella, I. 2017. Functional Modelling of High Lift Systems. *NAFEMS World Congress 2017*. NAFEMS, awaiting publication.
- Walden, D. 2015. INCOSE Systems Engineering Handbook 4th Ed. *INCOSE*. WILEY.
- SEBoK. 2017. Guide to the Systems Engineering Body of Knowledge – Validation and verification diagram, *sebokwiki.org*.
- ARP4754A, 2010, Guidelines for Development of Civil Aircraft and Systems, *SAE International*
- Zadeh, Desoer, 1963. “Linear System Theory – The State Space Approach” McGraw Hill, New York

APPENDIX

Table 1: Table of model parameters.

K_{hyd}	Hydraulic fluid bulk modulus
ρ_{hyd}	Hydraulic fluid density
I_{mot}	Hydraulic motor inertia
K_{mot}	Hydraulic motor displacement
T_s	Control valve time constant
A_{valve}	Control valve area
C_{valve}	Coefficient of discharge for control valve
P_{PDU}	PDU brake disengagement pressure
G_{PDU}	PDU gearbox ratio
η_{mot}	Motor efficiency
T_{drag_m}	Motor drag
k_{trans}	Transmission torsional stiffness
c_{trans}	Transmission torsional damping
η_{trans}	Transmission dynamic efficiency
T_{drag}	Transmission system drag
I_{act}	Actuator inertia
T_{OBB}	Outboard brake response time
P_{OBB}	Outboard brake disengagement pressure
G_{sensor}	Gear ratio position sensor
T_{aero}	Aerodynamic loads at all actuators
G_{act}	Gear ratios of rotary geared actuators
η_{act}	Actuator efficiency